DALTON

Structural, spectroscopic and redox studies of *trans*-$[RuX_2L_4]^{0/+}$ (L = PR_3, AsR_3 or SbR_3; X = Cl, Br or I). Crystal structures of *trans*-$[RuX_2(EMe_2Ph)_4]$ (X = Br, E = Sb; X = I, E = As), $[Ru_2Br_5(SbMe_2Ph)_4]$ and $[Ru_2I_3(PMe_2Ph)_6][CF_3SO_3]$

Nicholas J. Holmes, William Levason* and Michael Webster

Department of Chemistry, University of Southampton, Southampton, UK SO17 1BJ

The complexes *trans*-$[RuX_2L_4]$ (X = Cl, Br or I; L = PMe_3, $AsMe_2Ph$ or $SbMe_2Ph$) have been prepared from $RuCl_3{\cdot}nH_2O$, LiX and L, from $[Ru(dmf)_6][CF_3SO_3]_3$ (dmf = *N*,*N*-dimethylformamide), LiX and L, and in other ways. The complexes *cis*-$[RuX_2(PMe_2Ph)_4]$ (X = Cl or Br) have been made from $[RuX_2(PPh_3)_3]$ and PMe_2Ph in hexane and *cis*-$[RuX_2(PMe_3)_4]$ from solutions of the *trans* isomers on standing in CH_2Cl_2. Oxidation of *trans*-$[RuX_2L_4]$ to *trans*-$[RuX_2L_4]BF_4$ has been achieved either with $AgBF_4$ in CH_2Cl_2 or concentrated HNO_3 in aqueous HBF_4. The complexes have been characterised by analysis, UV/VIS, IR, ^1H and ^{31}P-$\{^1H\}$ NMR spectroscopy as appropriate, and the Ru^{II}–Ru^{III} oxidations probed by cyclic voltammetry. The behaviour of this series of complexes is compared with that of the osmium $[OsX_2L_4]^{0/+/2+}$ analogues. The crystal structures of *trans*-$[RuX_2L_4]$ (X = I, L = $AsMe_2Ph$; X = Br, L = $SbMe_2Ph$), $[Ru_2Br_5(SbMe_2Ph)_4]$ and $[Ru_2I_3(PMe_2Ph)_6][CF_3SO_3]$ have been determined.

We have described elsewhere the effects of systematic variation of both neutral and halide ligands upon the stability, spectroscopic properties and redox chemistry of several series of osmium complexes including *trans*-$[OsX_4L_2]^{0/-}$ (ref. 1), *mer*-$[OsX_3L_3]^{0/+}$ (ref. 2) and *trans*-$[OsX_2L_4]^{0/+/2+}$ (ref. 3) (L = PR_3, AsR_3 or SbR_3; X = Cl or Br, sometimes I). Limited information is available for ruthenium complexes with monodentate ligands, in part because of the much greater reactivity and their tendency to rearrange into halide-bridged dimers.[4–6] The studies of $[RuX_{6-n}(RCN)_n]$ are a notable contribution involving nitrogen donor ligands.[7] More recently we have observed that for *mer*-$[RuX_3L_3]$ both oxidation and reduction are electrochemically irreversible, and solution decomposition yields the Ru_2^{5+} species $[Ru_2X_5L_4]$.[8] Here we report studies of the tetrakis(ligand) complexes *trans*-$[RuX_2L_4]^{0/+}$ and *cis*-$[RuX_2(PR_3)_4]$.

Results and Discussion

Synthesis and properties of ruthenium(II) complexes

The complex *trans*-$[RuCl_2(PMe_3)_4]$ is best made from $[RuCl_2(PPh_3)_3]$ and PMe_3 in hexane,[6] whilst a similar reaction using PMe_2Ph affords *cis*-$[RuX_2(PMe_2Ph)_4]$ (X = Cl or Br).[4] For reasons that are unclear the reaction of $[RuX_2(PPh_3)_3]$ (X = Br or I) with PMe_3 in hexane did not cleanly afford *trans*-$[RuX_2(PMe_3)_4]$, and the latter were best made by reflux of *trans*-$[RuCl_2(PMe_3)_4]$ with the appropriate LiX in ethanol. The complexes *cis*-$[RuX_2(PMe_3)_4]$ (X = Cl or Br) have previously been prepared[6] by reduction of the *trans* isomers with Na/Hg to give $[RuH(\eta^2\text{-}CH_2PMe_2)(PMe_3)_3]$ followed by reaction with HX. A simpler preparation is to allow CH_2Cl_2 solutions of the *trans* isomers to stand for several days with exclusion of oxygen, when almost complete (>95%) conversion occurs as monitored by ^{31}P-$\{^1H\}$ NMR spectroscopy. These complexes are stable in CH_2Cl_2, but *cis*-$[RuX_2(PMe_2Ph)_4]$ rapidly rearrange into the dimers $[Ru_2(\mu\text{-}X)_3(PMe_2Ph)_6]X$ at ambient temperatures.[4] The reaction of $[RuI_2(PPh_3)_3]$[9] with PMe_2Ph in hexane affords a fawn solid, analytically $[RuI_2(PMe_2Ph)_4]$. A freshly prepared solution of this in cold (250 K) $CHCl_3$, exhibited a ^{31}P-$\{^1H\}$ NMR spectrum consisting of two broad signals (ill defined triplets?) of approximately 1:1 intensity at δ +2.1 and −29.4 attributed to *cis*-$[RuI_2(PMe_2Ph)_4]$ and a sharp singlet at δ +5.7, tentatively assigned to the *trans* isomer. However after 30 min at room temperature the solution had a ^{31}P-$\{^1H\}$ NMR spectrum which had completely lost these resonances, and now contained five singlets. It would seem that the rearrangement of $[RuI_2(PMe_2Ph)_4]$ is even faster than for the lighter halides, and the products of rearrangement have not been identified. Refluxing $[Ru(dmf)_6][CF_3SO_3]_3$[10] (dmf = *N*,*N*-dimethylformamide) with PMe_2Ph and LiI in ethanol produced the dimer $[Ru_2(\mu\text{-}I)_3(PMe_2Ph)_6][CF_3SO_3]$, which had a single ^{31}P-$\{^1H\}$ NMR resonance at δ +11.7, and was fully characterised by a single-crystal X-ray study (below). The arsine and stibine complexes *trans*-$[RuX_2L_4]$ (X = Cl, Br or I; L = $AsMe_2Ph$ or $SbMe_2Ph$) were made directly from $RuCl_3{\cdot}nH_2O$ and an excess of L in alcohols (with an excess of LiX in the case of X = Br or I). The iodo-complexes can also be made from $[Ru(dmf)_6][CF_3SO_3]_3$, L and LiI. Unlike the phosphines, the arsine and stibine complexes show no tendency to isomerise to the *cis* forms. Surprisingly few ruthenium iodo complexes have been characterised previously,[9] and the only tertiary stibine complexes in the literature are *trans*-$[RuX_2(SbPh_3)_4]$.[11]

The *trans*-$[RuX_2L_4]$ complexes which range from orange to red-purple (Table 1) were characterised by analysis and either electrospray or FAB mass spectrometry (Experimental section). The identification as *trans* isomers was made on the basis of single ^1H, and for L = PMe_3 single ^{31}P-$\{^1H\}$, NMR resonances, and this was confirmed by X-ray studies of *trans*-$[RuI_2(AsMe_2Ph)_4]$, *trans*-$[RuBr_2(SbMe_2Ph)_4]$ and *trans*-$[RuI_2(SbMe_2Ph)_4]$ (see below). The UV/VIS spectra (Table 1) typically show two moderate-intensity bands in the region 18 000–28 000 cm^{-1}, which may be assigned to the d–d transitions, $^1A_{1g} \longrightarrow {}^1E_g$ and $^1A_{1g} \longrightarrow {}^1A_{2g}$ respectively in D_{4h} symmetry.[12] For *trans*-$[RuX_2(PMe_3)_4]$ (X = Cl or Br) bands of similar intensity appear at *ca.* 30 000 cm^{-1} and may be derived from the $^1A_{1g} \longrightarrow {}^1T_{2g}$ transitions. For the other ruthenium(II) complexes (Table 1) the higher-energy bands have larger ε_{mol} values suggestive of charge-transfer or internal-ligand transitions. The complexes *trans*-$[RuX_2(PMe_3)_4]$ in CH_2Cl_2 slowly oxidise in air to Ru^{III}, but the other complexes are air-stable. Cyclic voltammetry reveals (Table 2) reversible one-electron oxidations occur in the range 0.4–0.7 V, similar to those of ruthenium(II) com-

Table 1 The UV/VIS spectral data of $[RuX_2L_4]$ and $[RuX_2L_4]BF_4$ in CH_2Cl_2 solutions

Complex	Colour	$E_{max}/10^3$ cm^{-1} (ε_{mol}/dm^3 mol^{-1} cm^{-1})
trans-$[RuCl_2(PMe_3)_4]$	Orange	32.1 (670), 27.3 (sh) (≈450), 22.5 (230)
trans-$[RuBr_2(PMe_3)_4]$	Orange	31.2 (730), 27.8 (330), 21.4 (225)
trans-$[RuI_2(PMe_3)_4]$	Pink	33.3 (11 300), 20.4 (520)
trans-$[RuCl_2(AsMe_2Ph)_4]$	Dark orange	33.9 (sh) (3200), 27.0 (sh) (≈400), 20.3 (380)
trans-$[RuBr_2(AsMe_2Ph)_4]$	Purple	30.0 (sh) (≈1000), 26.3 (sh) (≈400), 19.6 (290)
trans-$[RuI_2(AsMe_2Ph)_4]$	Purple	31.4 (11 300), 25.0 (sh) (≈500), 18.7 (260)
trans-$[RuCl_2(SbMe_2Ph)_4]$	Pink	35.6 (32 850), 25.6 (sh) (≈500), 19.5 (450)
trans-$[RuBr_2(SbMe_2Ph)_4]$	Purple-red	33.3 (sh) (18 000), 25.6 (sh) (≈450), 19.0 (385)
trans-$[RuI_2(SbMe_2Ph)_4]$	Red	33.9 (16 270), 29.3 (7100), 27.3 (sh), 18.6 (330)
cis-$[RuCl_2(PMe_3)_4]$	Yellow	29.3 (760)
cis-$[RuBr_2(PMe_3)_4]$	Yellow	28.5 (900)
cis-$[RuCl_2(PMe_2Ph)_4]$	Yellow	29.8 (2380), 27.3 (sh) (≈1900)
cis-$[RuBr_2(PMe_2Ph)_4]$	Yellow	29.0 (1480), 26.8 (sh) (≈1250)
trans-$[RuCl_2(PMe_3)_4]BF_4$	Green	27.5 (2970), 24.6 (sh) (≈900), 17.5 (sh) (≈600), 16.0 (1030)
trans-$[RuBr_2(PMe_3)_4]BF_4$	Green	23.5 (1965), 15.9 (580), 14.5 (1615)
trans-$[RuI_2(PMe_3)_4]BF_4$	Purple	30.5 (3435), 20.5 (1020), 17.7 (sh) (≈540), 12.8 (sh) (≈560), 11.2 (5400)
trans-$[RuCl_2(AsMe_2Ph)_4]BF_4$	Green	33.8 (27 100), 27.3 (sh) (≈2320), 24.4 (sh) (≈1200), 14.9 (1000)
trans-$[RuBr_2(AsMe_2Ph)_4]BF_4$	Green-brown	33.0 (18 190), 22.8 (1410), 13.6 (1335)
trans-$[RuI_2(AsMe_2Ph)_4]BF_4$	Brown	31.7 (sh) (8775), 24.9 (sh) (≈1460), 19.0 (870), 16.6 (740), 11.2 (930)
trans-$[RuCl_2(SbMe_2Ph)_4]BF_4$	Orange-brown	34.6 (21 300), 24.4 (1450), 18.6 (sh) (300), 12.9 (130)
trans-$[RuBr_2(SbMe_2Ph)_4]BF_4$	Brown	32.9 (18 400), 28.1 (19 000), 22.7 (sh) (≈1350), 18.8 (sh) (≈630), 11.0 (330)
trans-$[RuI_2(SbMe_2Ph)_4]BF_4$	Dark brown	30.7 (13 800), 26.5 (7700), 20.0 (1300), 11.0 (280), 9.2 (2100)

Table 2 Electrochemical data, E_e/V *vs.* SCE[a]

Complex	Ru^{II}–Ru^{III} [b]	Ru^{III}–Ru^{II} [c]
trans-$[RuCl_2(PMe_3)_4]^{0/+}$	0.44	0.45
trans-$[RuBr_2(PMe_3)_4]^{0/+}$ [d]	0.38	0.40
trans-$[RuI_2(PMe_3)_4]^{0/+}$	0.64	0.68
trans-$[RuCl_2(AsMe_2Ph)_4]^{0/+}$	0.56	0.56
trans-$[RuBr_2(AsMe_2Ph)_4]^{0/+}$	0.59	0.58
trans-$[RuI_2(AsMe_2Ph)_4]^{0/+}$	0.60	0.59
trans-$[RuCl_2(SbMe_2Ph)_4]^{0/+}$	0.64	0.63
trans-$[RuBr_2(SbMe_2Ph)_4]^{0/+}$	0.66	0.64
trans-$[RuI_2(SbMe_2Ph)_4]^{0/+}$	0.64	0.66
cis-$[RuCl_2(PMe_3)_4]$	1.25 [d,e]	—
cis-$[RuBr_2(PMe_3)_4]$	1.46 [d,e]	—

[a] In CH_2Cl_2 containing 0.2 mol dm^{-3} $[NBu^n_4][BF_4]$. Reversible couples with ΔE_p in the range 60–80 mV unless indicated otherwise. In this solvent ferrocene–ferrocenium occurs at 0.57 V. [b] Starting with $[RuX_2L_4]$ complex, forward process is oxidation. [c] Starting with $[RuX_2L_4]^+$ complex, forward process is reduction. [d] In MeCN *versus* ferrocene–ferrocenium at 0.41 V. [e] Irreversible.

plexes with diphosphine and diarsine ligands,[12] but approximately 0.3 V more positive than observed for the osmium analogues.[3] The effect on E_O of changing the halogen is very small, but the redox potentials shift to more positive values with the neutral donor $PR_3 < AsR_3 < SbR_3$.

The *cis* isomers were obtained only with PMe_3 and PMe_2Ph, the geometry being established by the presence of two triplets (1:1) in the ^{31}P-$\{^1H\}$ NMR spectra. The yellow *cis* isomers exhibit only a single weak d–d band sometimes with a low-energy shoulder <30 000 cm^{-1} (Table 1). In marked contrast to the *trans* analogues, *cis*-$[RuX_2(PMe_3)_4]$ show only an irreversible oxidation at much more positive potentials, a trend also seen in the osmium analogues.[3]

Crystal structures of *trans*-$[RuX_2(EMe_2Ph)_4]$ (X = Br, E = Sb; X = I, E = As) †

Both species adopt the *trans* geometry, the bromide is shown in Fig. 1 and the iodide in Fig. 2, with selected bond lengths and angles in Table 3. There is no crystallographic symmetry but the RuX_2E_4 framework is approximately D_{4h} [*cis* (90°) angles in the

† The structure of *trans*-$[RuI_2(SbMe_2Ph)_4]$ was also determined and found to be isomorphous with the arsine analogue. The data were not of good quality but established the *trans* geometry: $a = 17.884(3)$, $b = 9.439(8)$, $c = 23.233(2)$ Å, $\beta = 104.022(9)°$, space group $P2_1/a$, $Z = 4$, 150 K.

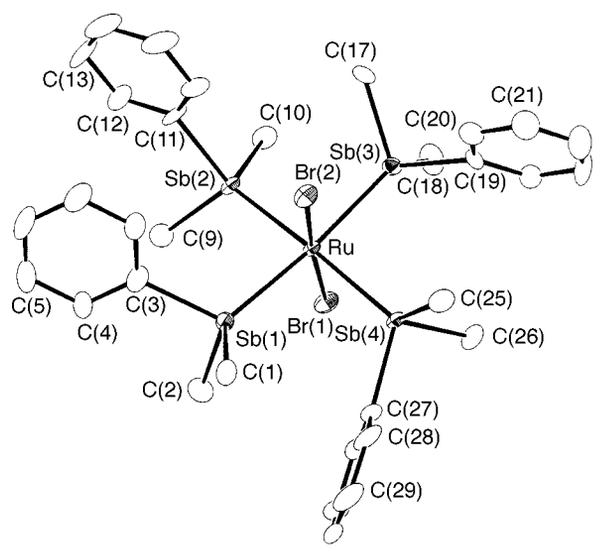

Fig. 1 Structure of *trans*-$[RuBr_2(SbMe_2Ph)_4]$ showing the atom labelling scheme. Hydrogen atoms are omitted for clarity and the thermal ellipsoids are drawn at the 50% probability level

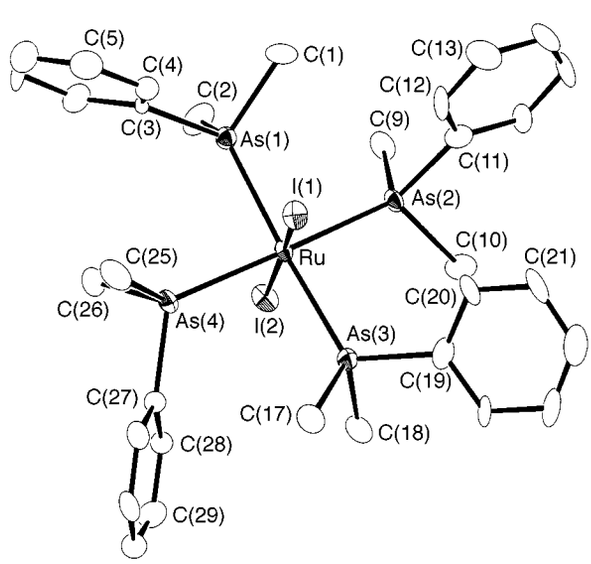

Fig. 2 Structure of *trans*-$[RuI_2(AsMe_2Ph)_4]$. Details as in Fig. 1

Table 3 Selected bond lengths (Å) and angles (°) for *trans*-$[RuX_2(EMe_2Ph)_4]$ (X = Br, E = Sb; X = I, E = As)

	X = Br, E = Sb	X = I, E = As
Ru–X(1)	2.572(1)	2.732(2)
Ru–X(2)	2.567(1)	2.745(2)
Ru–E(1)	2.590(1)	2.464(3)
Ru–E(2)	2.596(1)	2.504(2)
Ru–E(3)	2.573(1)	2.477(3)
Ru–E(4)	2.584(1)	2.458(2)
E–C	2.11(1)–2.16(1)	1.91(2)–1.97(2)
X(1)–Ru–X(2)	175.68(4)	174.61(6)
X–Ru–E (*cis*)	83.61(3)–100.01(3)	83.06(5)–101.65(6)
E–Ru–E (*cis*)	88.20(3)–92.62(3)	88.34(7)–93.39(7)
Ru–E–Me	115.0(3)–123.5(3)	115.7(5)–121.2(5)
Ru–E–Ph	115.4(3)–124.5(2)	120.0(5)–125.9(5)
C–E–C	95.5(4)–101.2(4)	95.1(6)–101.1(6)

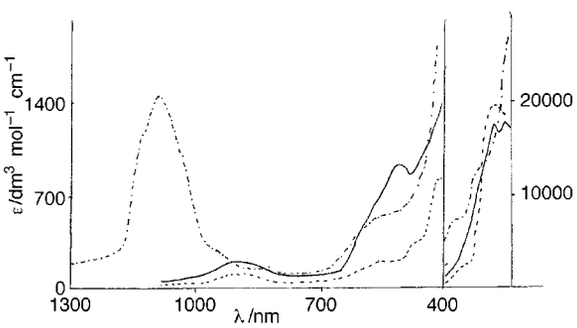

Fig. 3 The UV/VIS spectra of *trans*-$[RuX_2(SbMe_2Ph)_4]$ (X = Cl, Br or I) in CH_2Cl_2 solution (- - -, X = Cl; —, Br; - · -, I)

range 83.1–101.6°] with the conformation of the two methyl and phenyl groups dictated presumably by the inter- and intramolecular packing. The Ru–Sb distances in *trans*-$[RuCl_2(SbPh_3)_4]$[11] [2.625(1)–2.632(1) Å] are somewhat longer than the present values (Table 3). The ligand geometry is unexceptional.

Synthesis and properties of ruthenium(III) complexes

A variety of reagents were explored in attempts to oxidise the *trans*-$[RuX_2L_4]$ complexes. Halogens proved to be unsuitable tending to remove some L ligands. For *trans*-$[RuX_2L_4]$ (L = PMe_3 or $AsMe_2Ph$) oxidation to the ruthenium(III) complexes was achieved by $AgBF_4$ in CH_2Cl_2, but the reaction failed for L = $SbMe_2Ph$, and the arsine and stibine complexes were oxidised easily using concentrated HNO_3–HBF_4 at 0 °C. Given the highly positive redox potentials (Table 2), oxidation of *cis*-$[RuX_2(PR_3)_4]$ was expected to be difficult; in fact concentrated HNO_3 at 0 °C rapidly converted the orange ruthenium(II) complexes into dark green materials, which turned brown and decomposed unless rapidly isolated. However examination of the green product formed from *cis*-$[RuCl_2(PMe_2Ph)_4]$ indicated that a nitrosyl complex [ν(NO) at 1838 cm^{-1}] was formed, and the reactions were not further studied.

The intensely coloured *trans*-$[RuX_2L_4]BF_4$ (Table 1) are stable in the solid state, and decompose only very slowly in chlorocarbon solvents. The *trans* geometry of these paramagnetic complexes is confirmed by the single ν(Ru–X) vibrations in the far-IR spectra, and by the cyclic voltammograms which showed reversible one-electron reductions to reform the ruthenium(II) complexes (Table 2). For *trans*-$[RuX_2(L–L)_2]^+$ [L–L for example *o*-$C_6H_4(PMe_2)_2$ or $Me_2PCH_2CH_2PMe_2$] irreversible oxidation at highly positive potentials to ruthenium(IV) complexes were observed, but these proved too unstable to isolate by chemical oxidation.[12] However for the less robust $[RuX_2L_4]^+$ complexes, only ill defined oxidations near to the solvent limit were evident in the cyclic voltammograms. The *trans*-$[RuX_2L_4]^+$ complexes have rich UV/VIS spectra (Table 1, Fig. 3), the main features of which can be assigned as L(σ)→Ru(t_{2g}) and X(π)→Ru(t_{2g}) charge transfer by analogy with the osmium(III) analogues.[3] In D_{4h} symmetry the ruthenium d orbitals split giving the configuration $b_2^2 < e^3 < a_1^0 < b_1^0$. From the reported spectra[12,13] of other *trans*-$[RuX_2L_4]^+$ we expect Cl(π)→Ru(e) at *ca.* 27 000 cm^{-1} and Br(π)→Ru(e) at *ca.* 22 000 cm^{-1}, with I(π)→Ru(e) at *ca.* 12 000–10 000 cm^{-1},[9] whilst other low-energy features will be P/As/Sb(σ)→Ru(e), Ru(a_1). The spectra are complex and as we have argued elsewhere[3,12] are complicated by near coincidence of some transitions and the increasing splitting produced by spin–orbit effects in complexes with the heavier donors. As usual corresponding features shift to low energy by 3000–5000 cm^{-1} between Os and Ru reflecting the greater ease of reduction in the ruthenium(III) systems.

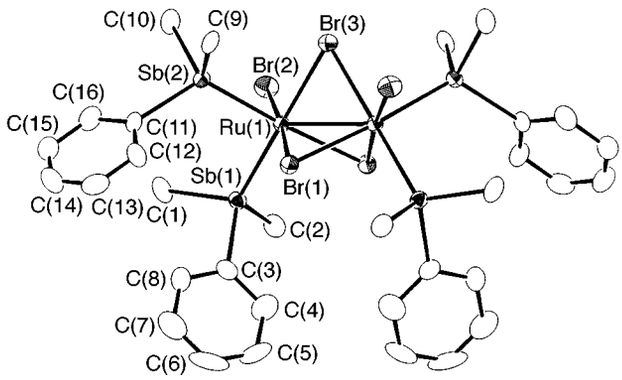

Fig. 4 Structure of $[Ru_2Br_5(SbMe_2Ph)_4]$. Details as in Fig. 1

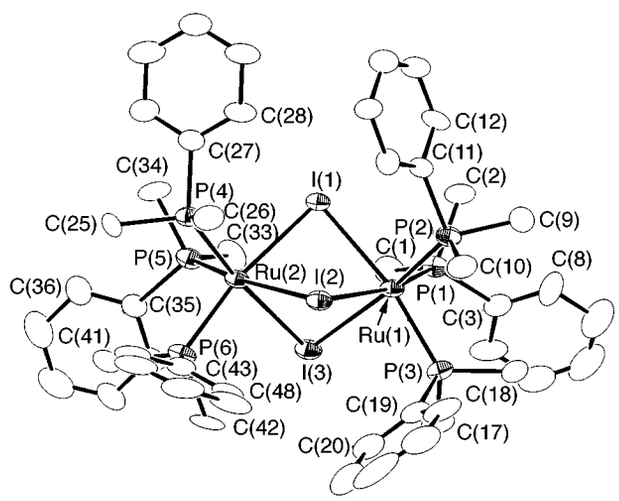

Fig. 5 Structure of the cation in $[Ru_2I_3(PMe_2Ph)_6][CF_3SO_3]$. Details as in Fig. 1

Structures of $[Ru_2Br_5(SbMe_2Ph)_4]$ and $[Ru_2I_3(PMe_2Ph)_6][CF_3SO_3]$

The structures of the binuclear $[Ru_2Br_5(SbMe_2Ph)_4]$ and the cation $[Ru_2I_3(PMe_2Ph)_6]^+$ are shown in Figs. 4 and 5 respectively and selected bond lengths and angles are given in Table 4. Both species contain the well known confacial bioctahedral arrangement with three bridging halogen atoms. A few X-ray-quality crystals of the former arose during attempts to grow crystals of $[RuBr_2(SbMe_2Ph)_4]$. The complex $[Ru_2Br_5(SbMe_2Ph)_4]$ has two-fold crystallographic symmetry and is isomorphous with the analogous compounds of P and As recently reported.[8] It appears to represent the first Ru_2^{5+} derivative with an antimony ligand. The Ru–Ru distance [2.942(2) Å] is similar to the value in the corresponding arsine compound[8] and it is regarded as having a bond-order of 0.5. In the second compound, $[Ru_2I_3(PMe_2Ph)_6][CF_3SO_3]$, the cation has no crystallo-

Table 4 Selected bond lengths (Å) and angles (°) for $[Ru_2Br_5(SbMe_2Ph)_4]$ and $[Ru_2I_3(PMe_2Ph)_6][CF_3SO_3]$

(*a*) $[Ru_2Br_5(SbMe_2Ph)_4]$

Ru–Br(1)	2.516(2)	Ru–Ru′	2.942(2)
Ru–Br(1′)	2.582(2)	Ru–Sb(1)	2.558(2)
Ru–Br(2)	2.503(2)	Ru–Sb(2)	2.548(2)
Ru–Br(3)	2.592(2)	Sb–C	2.11(1)–2.15(1)
Ru–Br(1)–Ru′	70.48(6)	Br(1′)–Ru–Sb(2)	174.03(6)
Ru–Br(3)–Ru′	69.17(7)	Br(3)–Ru–Sb(1)	173.37(6)
Br(1)–Ru–Br(2)	175.33(7)	Sb(1)–Ru–Sb(2)	97.63(5)
Ru–Sb–C	112.9(4)–122.0(4)	C–Sb–C	98.6(5)–102.9(6)

(*b*) $[Ru_2I_3(PMe_2Ph)_6][CF_3SO_3]$

Ru(1)–I(1)	2.794(5)	Ru(1)–P(1)	2.320(14)
Ru(1)–I(2)	2.769(19)	Ru(1)–P(2)	2.299(4)
Ru(1)–I(3)	2.782(2)	Ru(1)–P(3)	2.328(5)
Ru(2)–I(1)	2.787(8)	Ru(2)–P(4)	2.315(12)
Ru(2)–I(2)	2.795(2)	Ru(2)–P(5)	2.304(5)
Ru(2)–I(3)	2.806(15)	Ru(2)–P(6)	2.347(7)
P–C	1.81(2)–1.87(2)	Ru(1) · · · Ru(2)	3.740(18)
Ru(1)–I(1)–Ru(2)	84.2(3)	I(1)–Ru(1)–I(2)	79.2(3)
Ru(1)–I(2)–Ru(2)	84.5(2)	I(1)–Ru(1)–I(3)	81.5(1)
Ru(1)–I(3)–Ru(2)	84.0(2)	I(2)–Ru(1)–I(3)	79.9(1)
I(1)–Ru(2)–I(2)	78.83(6)	I(2)–Ru(2)–I(3)	79.09(7)
I(1)–Ru(2)–I(3)	81.2(4)	P–Ru–P	92.2(4)–98.9(2)
Ru–P–C	113.8–123.4(6)	C–P–C	96.7(9)–102.0(8)

Symmetry operation: (′) $1 - x, y, \frac{1}{2} - z$.

graphic symmetry and the bridging iodine atoms are bonded symmetrically [Table 4(*b*)]. The counter ion was modelled as an extensively disordered triflate anion, $[CF_3SO_3]^-$ (see Experimental section). Several comparable structures of the type $[Ru_2X_3(ER_3)_6]^+$ have been reported (for a summary see ref. 14); the Ru · · · Ru distance [3.74(2) Å], which is 0.4 Å longer than in the chloro compound, indicates that there is no bond present, and this example appears to be the first iodo derivative structurally characterised.

Conclusion

This is the first systematic study of a series of redox pairs *trans*-$[RuX_2L_4]^{0/+}$, and it is useful to compare the results with previous data on the osmium analogues.[3] There are considerable similarities, *e.g.* the isomerisation of *trans*-$[MX_2(PR_3)_4]$ to *cis*-$[MX_2(PR_3)_4]$ (M = Ru or Os) in chlorocarbon solution, although for *cis*-$[OsX_2(PMe_2Ph)_4]$ further rearrangement into dimers is not observed at ambient temperatures. For both metals, oxidation of the *trans* isomers is much easier than for the *cis*, and comparison of the redox potentials shows that Os^{II}–Os^{III} couples are typically 0.3–0.5 V less positive than for Ru^{II}–Ru^{III} for the same ligand set. Moreover further reversible oxidation to Os^{IV} is often observed,[3] whereas there is no evidence that ruthenium(IV) complexes can be formed. As in the *mer*-$[RuX_3L_3]$ systems,[7] the formation of halide-bridged dimers is relatively facile for the ruthenium systems, whereas the corresponding osmium complexes form only slowly under much more forcing conditions.[5]

Experimental

Physical measurements were made as described previously.[2,8]

Ruthenium(II) complexes

***trans*-[RuCl$_2$(AsMe$_2$Ph)$_4$].** The compounds $RuCl_3 \cdot xH_2O$ (0.5 g, 1.9 mmol) and $AsMe_2Ph$ (1.81 g, 9.95 mmol) in methanol (25 cm^3) were refluxed under nitrogen for 17 h and then cooled to room temperature. The dark orange solid obtained was filtered off, washed with methanol (2 × 15 cm^3), and dried *in vacuo* (1.3 g, 76% based on $RuCl_3 \cdot xH_2O$) (Found: C, 42.4; H, 4.6. Calc. for $C_{32}H_{44}As_4Cl_2Ru$: C, 42.7; H, 4.9%). $\tilde{\nu}$(Ru–Cl)/cm^{-1} (Nujol mull) 304. Electrospray mass spectrum: *m*/*z* 717 and 682. Calc. for $C_{24}H_{33}As^{35}Cl_2{}^{101}Ru$ 717, $C_{24}H_{33}As_3{}^{35}Cl^{101}Ru$ 682. ^{1}H NMR (298 K, $CDCl_3$): δ 1.35 (s) and 7.0–7.6 (m).

***trans*-[RuBr$_2$(AsMe$_2$Ph)$_4$].** The compounds $RuCl_3 \cdot xH_2O$ (0.38 g, 1.45 mmol) and LiBr (2.25 g, 25.9 mmol) in water (100 cm^3) were refluxed under nitrogen for 2 h and then stirred at room temperature overnight. The water was removed (hot-plate stirrer) and methanol (30 cm^3) and $AsMe_2Ph$ (1.38 g, 7.58 mmol) were added. The mixture was then refluxed under nitrogen for 17 h and cooled to room temperature. The purple solid obtained was filtered off, washed with methanol (2 × 15 cm^3), and dried *in vacuo* (1.3 g, 91% based on $RuCl_3 \cdot xH_2O$) (Found: C, 38.6; H, 4.4. Calc. for $C_{32}H_{44}As_4Br_2Ru$: C, 38.8; H, 4.5%). $\tilde{\nu}$(Ru–Br)/cm^{-1} (Nujol mull) 248. Electrospray mass spectrum: *m*/*z* = 807, 726. Calc. for $C_{24}H_{33}As_3{}^{79}Br_2{}^{101}Ru$ 805, $C_{24}H_{33}As_3{}^{79}Br^{101}Ru$ 726. ^{1}H NMR (298 K, $CDCl_3$): δ 1.5 (s) and 7.1–7.7 (m).

***trans*-[RuI$_2$(AsMe$_2$Ph)$_4$].** The complex $[Ru(dmf)_6][CF_3SO_3]_3$[10] (0.67 g, 0.68 mmol) was dissolved in warm ethanol (30 cm^3). To this, $AsMe_2Ph$ (0.37 g, 2.03 mmol) was added and the mixture heated to reflux under nitrogen for 30 min. To the dark yellow solution formed, LiI (0.31 g, 2.04 mmol) in ethanol (10 cm^3) was added and the mixture again heated to reflux under nitrogen for 15 min. On cooling a light purple solid separated from the light purple solution and was filtered off, washed with diethyl ether (2 × 15 cm^3), and dried *in vacuo* (0.47 g, 64%) (Found: C, 35.6; H, 3.0. Calc. for $C_{32}H_{44}As_4I_2Ru$: C, 36.0; H, 4.1%). Electrospray mass spectrum: *m*/*z* = 901, 774, 718 and 647. Calc. for $C_{24}H_{33}As_3I_2{}^{101}Ru$ 901, $C_{24}H_{33}As_3I^{101}Ru$ 774, $C_{16}H_{22}As_2I_2{}^{101}Ru$ 719 and $C_{24}H_{33}As_3{}^{101}Ru$ 647. ^{1}H NMR (298 K, $CDCl_3$): δ 1.6 (s) and 7.1–7.8 (m).

***trans*-[RuCl$_2$(SbMe$_2$Ph)$_4$].** The compounds $RuCl_3 \cdot xH_2O$ (0.35 g, 1.34 mmol) and $SbMe_2Ph$ (1.24 g, 5.41 mmol) in ethanol (30 cm^3) containing concentrated HCl (1 cm^3) were heated to reflux under nitrogen. The mixture was then immediately cooled to room temperature and stirred at room temperature for 1 h. The pink solid formed was filtered from the deep green solution, washed with ethanol (2 × 15 cm^3), and dried *in vacuo* (0.30 g, 21%). It was recrystallised from dichloromethane–ethanol (Found: C, 34.6; H, 3.8. Calc. for $C_{32}H_{44}Cl_2RuSb_4$: C, 35.2; H, 4.0%). FAB mass spectrum: *m*/*z* = 1087, 1052, 859, 824 and 630. Calc. for $C_{32}H_{44}{}^{35}Cl_2{}^{101}Ru^{121}Sb_4$ 1083, $C_{32}H_{44}{}^{35}Cl^{101}Ru^{121}Sb_4$ 1048, $C_{24}H_{33}{}^{35}Cl_2{}^{101}Ru^{121}Sb_3$ 855, $C_{24}H_{33}{}^{35}Cl^{101}Ru^{121}Sb_3$ 820 and $C_{16}H_{22}{}^{35}Cl_2{}^{101}Ru^{121}Sb_2$ 627. ^{1}H NMR (298 K, $CDCl_3$): δ 1.15 (s) and 7.1–7.6 (m).

***trans*-[RuBr$_2$(SbMe$_2$Ph)$_4$].** The compounds $RuCl_3 \cdot xH_2O$ (0.25 g, 0.96 mmol) and LiBr (1.50 g, 17.24 mmol) in water (40 cm^3) were refluxed under nitrogen for 2 h and then stirred at room temperature overnight. The water was removed and ethanol (30 cm^3), $SbMe_2Ph$ (0.57 g, 2.49 mmol) and concentrated HBr (1 cm^3) were added. The mixture was heated to reflux then immediately cooled to room temperature and stirred for 1 h. The purple solid obtained was filtered off, washed with ethanol (2 × 15 cm^3), and dried *in vacuo* (0.44 g, 39%). It was recrystallised from dichloromethane–ethanol to give red–purple crystals (Found: C, 32.6; H, 4.0. Calc. for $C_{32}H_{44}Br_2RuSb_4$: C, 32.6; H, 3.7%). FAB mass spectrum: *m*/*z* = 1175, 1096, 947, 868 and 719. Calc. for $C_{32}H_{44}{}^{79}Br_2{}^{101}Ru^{121}Sb_4$ 1171, $C_{32}H_{44}{}^{79}Br^{101}Ru^{121}Sb_4$ 1092, $C_{24}H_{33}{}^{79}Br_2{}^{101}Ru^{121}Sb_3$ 943, $C_{24}H_{33}$-

$^{79}Br^{101}Ru^{121}Sb_3$ 864 and $C_{16}H_{22}{}^{79}Br_2{}^{101}Ru^{121}Sb_2$ 715. ^1H NMR (298 K, $CDCl_3$): δ 1.2 (s) and 7.1–7.6 (m).

***trans*-[RuI$_2$(SbMe$_2$Ph)$_4$].** The compounds $RuCl_3{\cdot}xH_2O$ (0.25 g, 0.96 mmol) and LiI (2.29 g, 15.07 mmol) in water (30 cm^3) were refluxed under nitrogen for 2 h and then stirred at room temperature overnight. The water was removed and ethanol (30 cm^3), $SbMe_2Ph$ (0.52 g, 22.7 mmol) and HI (57%, 1 cm^3) were added. The mixture was heated to reflux then immediately cooled to room temperature and stirred for 1 h. The dark brown solid obtained was filtered off, washed with ethanol (2 × 15 cm^3), and dried *in vacuo* (0.40 g, 33%). It was recrystallised from dichloromethane–ethanol to give red crystals (Found: C, 30.0; H, 3.7. Calc. for $C_{32}H_{44}I_2RuSb_4$: C, 30.2; H, 3.5%). FAB mass spectrum: *m*/*z* = 1271, 1144, 1041, 914, 813 and 686. Calc. for $C_{32}H_{44}I_2{}^{101}Ru^{121}Sb_4$ 1267, $C_{32}H_{44}I^{101}Ru^{121}Sb_4$ 1140, $C_{24}H_{33}I_2{}^{101}Ru^{121}Sb_3$ 1039, $C_{24}H_{33}I^{101}Ru^{121}Sb_3$ 912, $C_{16}H_{22}I_2{}^{101}Ru^{121}Sb_2$ 811 and $C_{16}H_{22}I^{101}Ru^{121}Sb_2$ 684. ^1H NMR (298 K, $CDCl_3$): δ 1.3 (s) and 7.1–7.7 (m).

[Ru$_2$I$_3$(PMe$_2$Ph)$_6$][CF$_3$SO$_3$]. The complex $[Ru(dmf)_6][CF_3SO_3]_3$ [10] (1.15 g, 1.17 mmol) was dissolved in warm ethanol (30 cm^3). To this PMe_2Ph (0.48 g, 3.50 mmol) was added and the mixture heated to reflux under nitrogen for 30 min. The red solution initially formed gradually turned yellow. To this LiI (0.53 g, 3.5 mmol) in ethanol (10 cm^3) was added and the mixture again heated to reflux under nitrogen for 50 min. On cooling a small amount of brown solid separated from an orange-brown solution. After filtering the orange-brown filtrate was reduced in volume to *ca.* 5 cm^3 and diethyl ether (50 cm^3) added to give a shiny light brown solid. This was washed with diethyl ether (2 × 15 cm^3) and dried *in vacuo* (0.60 g, 66%) (Found: C, 37.2; H, 4.2. Calc. for $C_{49}H_{66}F_3I_3O_3P_6Ru_2S$: C, 37.7; H, 4.2%). Electrospray mass spectrum: *m*/*z* = 1412, 1274 and 1136. Calc. for $C_{48}H_{66}I_3P_6{}^{101}Ru_2$ 1411, $C_{40}H_{55}I_3P_5{}^{101}Ru_2$ 1273 and $C_{32}H_{44}I_3P_4{}^{101}Ru_2$ 1135. ^{31}P-{^1H} NMR: δ 11.7 (s).

The complex *trans*-[RuCl$_2$(PMe$_3$)$_4$] was made according to the literature methods [6] from $[RuCl_2(PPh_3)_3]$ and PMe_3. ^{31}P-{^1H} NMR (298 K, CH_2Cl_2): δ −8.7 (s). ^1H NMR (298 K, $CDCl_3$): δ 1.4 (m).

***trans*-[RuBr$_2$(PMe$_3$)$_4$].** A solution of *trans*-[RuCl$_2$(PMe$_3$)$_4$] (0.20 g, 0.42 mmol) and LiBr (0.73 g, 8.4 mmol) was refluxed in ethanol (30 cm^3) for 12 h. The orange solution was filtered and reduced in volume to *ca.* 10 cm^3 when an orange solid separated. This was recrystallised from CH_2Cl_2–hexane, and dried *in vacuo* (0.1 g, 42%) (Found: C, 25.3; H, 6.0. Calc. for $C_{12}H_{36}Br_2P_4Ru$: C, 25.5; H, 6.4%). ^{31}P-{^1H} NMR (298 K, CH_2Cl_2): δ −10.7 (s). ^1H NMR (298 K, $CDCl_3$): δ 1.6 (m). Electrospray mass spectrum: *m*/*z* = 566, 490. Calc. for $C_{12}H_{36}{}^{79}Br_2P_4{}^{101}Ru$ 563, $C_9H_{27}{}^{79}BrP_3{}^{101}Ru$ 487.

The complex *trans*-[RuI$_2$(PMe$_3$)$_4$] was prepared similarly from *trans*-[RuCl$_2$(PMe$_3$)$_4$] and LiI in ethanol. The light pink product was recrystallised from CH_2Cl_2–hexane (76%) (Found: C, 21.9; H, 5.4. Calc. for $C_{12}H_{36}I_2P_4Ru$: C, 21.9; H, 5.5%). ^{31}P-{^1H} NMR (298 K, $CHCl_3$): δ −18.5 (s). ^1H NMR (298 K, $CDCl_3$): δ 1.74 (m). Electrospray mass spectrum: *m*/*z* = 659, 584. Calc. for $C_{12}H_{36}I_2P_4{}^{101}Ru$ 659, $C_9H_{27}I_2P_3{}^{101}Ru$ 584.

***cis*-[RuCl$_2$(PMe$_3$)$_4$].** A solution of the *trans* isomer in CH_2Cl_2 was allowed to stand under argon for 2 weeks. The solvent was removed in vacuum, and the solid rinsed with diethyl ether, recrystallised from CH_2Cl_2, and dried *in vacuo*. ^{31}P-{^1H} NMR (298 K, CD_2Cl_2): δ −12.7 (t) and +9.0 (t), *J* = 30 Hz. ^1H NMR (298 K, $CDCl_3$): δ 1.55 (m) and 1.50 (m). The complex *cis*-[RuBr$_2$(PMe$_3$)$_4$] was made similarly from the *trans* isomer. ^{31}P-{^1H} NMR (298 K, CH_2Cl_2): δ 10.3 (t) and −17.0 (t), *J* = 35 Hz. ^1H NMR (298 K, CD_2Cl_2): δ 1.65 (m) and 1.55 (m).

The complex *cis*-[RuCl$_2$(PMe$_2$Ph)$_4$] was made according to the literature method [4] (Found: C, 52.9; H, 5.8. Calc. for $C_{32}H_{44}Cl_2P_4Ru$: C, 53.0; H, 6.1%). Electrospray mass spectrum: *m*/*z* = 691. Calc. for $C_{32}H_{44}{}^{35}ClP_4{}^{101}Ru$ 688. ^{31}P-{^1H} NMR (220 K, $CDCl_3$): δ −9.1 (t) and +12.5 (t), *J* = 30 Hz.

The complex *cis*-[RuBr$_2$(PMe$_2$Ph)$_4$] was made according to the literature method [4] (Found: C, 47.3; H, 5.2. Calc. for $C_{32}H_{44}Br_2P_4Ru$: C, 47.2; H, 5.4%). Electrospray mass spectrum: *m*/*z* = 595. Calc. for $C_{24}H_{33}{}^{79}BrP_3{}^{101}Ru$ 594. ^{31}P-{^1H} NMR (260 K, $CDCl_3$): δ −15.3 (t) and +11.2 (t), *J* = 30 Hz.

[RuI$_2$(PMe$_2$Ph)$_4$]. The complex $[RuI_2(PPh_3)_3]$ [9] (0.037 g, 0.003 mmol) in degassed light petroleum (b.p. 60–80 °C, 40 cm^3) was stirred under nitrogen with PMe_2Ph (0.07 g, 0.50 mmol) for 1 h. The fawn solid was filtered off (Schlenk tube), washed with degassed light petroleum (2 × 15 cm^3) and dried *in vacuo* (0.023 g, 79%) (Found: C, 42.0; H, 5.3. Calc. for $C_{32}H_{44}I_2P_4Ru$: C, 42.3; H, 4.9%). ^{31}P-{^1H} NMR (250 K, $CHCl_3$): δ +2.1 and −29.4 (triplets?), +5.7 (s) (see text).

Ruthenium(III) complexes

***trans*-[RuCl$_2$(PMe$_3$)$_4$]BF$_4$.** The complex *trans*-[RuCl$_2$(PMe$_3$)$_4$] (0.10 g, 0.21 mmol) was dissolved in dichloromethane (5 cm^3). To this, $AgBF_4$ (0.04 g, 0.21 mmol) was added and the mixture stirred under nitrogen for 10 min to give a green solution, which was filtered. The filtrate was reduced in volume to *ca.* 3 cm^3 and hexane (25 cm^3) added to give a green solid which was filtered off, washed with hexane (2 × 10 cm^3) and dried *in vacuo* (0.051 g, 43%) (Found: C, 25.8; H, 4.5. Calc. for $C_{12}H_{36}BCl_2F_4P_4Ru$: C, 25.6; H, 4.6%). Electrospray mass spectrum: *m*/*z* = 443, 406 and 365. Calc. for $C_{12}H_{36}{}^{35}ClP_4{}^{101}Ru$ 440, $C_{12}H_{36}P_4{}^{101}Ru$ 405 and $C_9H_{27}{}^{35}ClP_3{}^{101}Ru$ 367.

The complex *trans*-[RuBr$_2$(PMe$_3$)$_4$]BF$_4$ was prepared similarly (47%) (Found: C, 21.6; H, 5.6. Calc. for $C_{12}H_{36}BBr_2F_4P_4Ru$: C, 22.1; H, 5.5%). Electrospray mass spectrum: *m*/*z* = 565, 490. Calc. for $C_{12}H_{36}{}^{79}Br_2P_4{}^{101}Ru$ 565, $C_9H_{27}{}^{79}Br_2P_3{}^{101}Ru$ 490.

The complex *trans*-[RuI$_2$(PMe$_3$)$_4$]BF$_4$ was made similarly (48%) (Found: C, 19.5; H, 5.0. Calc. for $C_{12}H_{36}BF_4I_2P_4Ru$: C, 19.3; H, 4.8%). Electrospray mass spectrum: *m*/*z* = 659, 584. Calc. for $C_{12}H_{36}I_2P_4{}^{101}Ru$ 659, $C_9H_{27}I_2P_3{}^{101}Ru$ 584.

***trans*-[RuCl$_2$(AsMe$_2$Ph)$_4$]BF$_4$.** The complex *trans*-[RuCl$_2$(AsMe$_2$Ph)$_4$] (0.135 g, 0.15 mmol) was dissolved in dichloromethane (5 cm^3). To this solution, $AgBF_4$ (0.03 g, 0.15 mmol) was added and the mixture stirred under nitrogen for 30 min to give a dark green solution, which was filtered. The filtrate was reduced in volume to *ca.* 3 cm^3 and hexane (25 cm^3) added to give a dark green solid which was filtered off, washed with hexane (2 × 10 cm^3) and dried *in vacuo* (0.08 g, 54%) (Found: C, 38.2; H, 3.9. Calc. for $C_{32}H_{44}As_4BCl_2F_4Ru$: C, 38.9; H, 4.5%). $\tilde{\nu}$(Ru–Cl)/cm^{-1} (Nujol mull) 332. Electrospray mass spectrum: *m*/*z* = 717, 681 and 538. Calc. for $C_{24}H_{33}As_3{}^{35}Cl_2{}^{101}Ru$ 717, $C_{24}H_{33}As_3{}^{35}Cl^{101}Ru$ 682 and $C_{16}H_{22}As_2{}^{35}Cl_2{}^{101}Ru$ 535.

***trans*-[RuBr$_2$(AsMe$_2$Ph)$_4$]BF$_4$.** The complex *trans*-[RuBr$_2$(AsMe$_2$Ph)$_4$] (0.15 g, 0.15 mmol) was dissolved in dichloromethane (5 cm^3). To this, $AgBF_4$ (0.03 g, 0.15 mmol) was added and the mixture stirred under nitrogen for 30 min to give a dark green solution, which was filtered. The filtrate was reduced in volume to *ca.* 3 cm^3 and hexane (25 cm^3) added to give a green-brown solid which was filtered off, washed with hexane (2 × 10 cm^3) and dried *in vacuo* (0.15 g, 93%) (Found: C, 35.9; H, 3.8. Calc. for $C_{32}H_{44}As_4BBr_2F_4Ru$: C, 35.7; H, 4.1%). $\tilde{\nu}$(Ru–Br)/cm^{-1} (Nujol mull) 254. Electrospray mass spectrum: *m*/*z* = 805, 726 and 624. Calc. for $C_{24}H_{33}As_3{}^{79}Br_2{}^{101}Ru$ 805, $C_{24}H_{33}As_3{}^{79}Br^{101}Ru$ 726 and $C_{12}H_{22}As_2{}^{79}Br_2{}^{101}Ru$ 623.

***trans*-[RuCl$_2$(SbMe$_2$Ph)$_4$]BF$_4$.** The complex *trans*-[RuCl$_2$(SbMe$_2$Ph)$_4$] was suspended in 40% HBF_4 (20 cm^3) in an ice-bath. To this, concentrated HNO_3 was added dropwise (several drops) and the mixture stirred for *ca.* 30 min. The orange-

Table 5 Crystallographic details for *trans*-$[RuX_2(EMe_2Ph)_4]$ (X = Br, E = Sb; X = I, E = As), $[Ru_2Br_5(SbMe_2Ph)_4]$ and $[Ru_2I_3(PMe_2Ph)_6][CF_3SO_3]$ *

	$[RuBr_2(SbMe_2Ph)_4]$	$[RuI_2(AsMe_2Ph)_4]$	$[Ru_2Br_5(SbMe_2Ph)_4]$	$[Ru_2I_3(PMe_2Ph)_6][CF_3SO_3]$
Molecular formula	$C_{32}H_{44}Br_2RuSb_4$	$C_{32}H_{44}As_4I_2Ru$	$C_{32}H_{44}Br_5Ru_2Sb_4$	$C_{49}H_{66}F_3I_3O_3P_6Ru_2S$
M_r	1176.58	1083.27	1517.36	1560.81
Crystal system	Triclinic	Monoclinic	Monoclinic	Triclinic
Space group	$P\bar{1}$ (no. 2)	$P2_1/a$ (no. 14)	$C2/c$ (no. 15)	$P\bar{1}$ (no. 2)
a/Å	13.034(4)	17.329(19)	16.048(7)	15.224(4)
b/Å	13.234(2)	9.282(48)	12.009(7)	18.957(6)
c/Å	11.896(3)	22.838(10)	21.881(7)	11.390(4)
α/°	103.97(2)			106.93(3)
β/°	105.44(2)	105.29(6)	99.75(3)	101.32(3)
γ/°	95.46(2)			73.72(2)
U/Å^3	1891.4(9)	3543(19)	4156(3)	2995.0 (1.7)
2θ range for cell/°	49.3–50.0	33.9–40.4	18.8–23.0	18.8–21.0
D_c/g cm^{-3}	2.066	2.031	2.425	1.724
Z	2	4	4	2
F(000)	1108	2072	2812	1528
Crystal size/mm	0.55 × 0.45 × 0.40	0.55 × 0.25 × 0.15	0.30 × 0.30 × 0.03	0.4 × 0.3 × 0.2
Total no. observations	6974	6901	3990	10 995
No. unique observations (R_{int})	6654 (0.015)	6669 (0.13)	3838 (0.080)	10 561 (0.08)
Absorption correction	ψ Scan	ψ Scan	ψ Scan	ψ Scan
Maximum, minimum transmission	0.553, 1.000	0.556, 1.000	0.360, 1.000	0.848, 1.000
No. data in refinement	5989 [$I > 2.5\sigma(I)$]	3794 [$I > 3\sigma(I)$]	2102 [$I > 2.5\sigma(I)$]	7169 [$I > 3\sigma(I)$]
No. parameters	352	332	195	560
μ/cm^{-1}	53.44	59.15	80.61	22.84
hkl Limits	0–15, −15 to 15, −14 to 13	0–20, 0–11, −27 to 26	0–19, 0–14, −25 to 25	0–18, −21 to 22, −13 to 13
S	3.56	2.38	1.55	4.11
Maximum shift/e.s.d.	0.12	0.03	0.02	0.22
Residual electron density/e Å^{-3}	1.73 to −3.15	1.65 to −1.82	1.54 to −1.27	2.13 to −1.70
R	0.047	0.049	0.041	0.060
R'	0.062	0.058	0.043	0.079

* Details in common: scan mode ω–2θ, $w^{-1} = \sigma^2(F_o)$; $2\theta_{max}$ 50.0°; T = 150 K; $R = \Sigma||F_o| - |F_c||/\Sigma|F_o|$; $R' = [\Sigma w(F_o - F_c)^2/\Sigma wF_o^2]^{\frac{1}{2}}$.

brown solid formed was filtered off, washed with water (2 × 10 cm^3) and dried *in vacuo* (Found: C, 33.7; H, 3.3. Calc. for $C_{32}H_{44}BCl_2F_4RuSb_4$: C, 32.7; H, 3.7%). Electrospray mass spectrum: m/z = 1053, 860 and 823. Calc. for $C_{32}H_{44}$-$^{35}Cl^{101}Ru^{121}Sb_4$ 1048, $C_{24}H_{33}{}^{35}Cl_2{}^{101}Ru^{121}Sb_3$ 855 and $C_{24}H_{33}$-$^{35}Cl^{101}Ru^{121}Sb_3$ 820.

The following complexes were prepared similarly: *trans*-$[RuBr_2(SbMe_2Ph)_4]BF_4$, brown solid (Found: C, 30.3; H, 3.6. Calc. for $C_{32}H_{44}BBr_2F_4RuSb_4$: C, 30.4; H, 3.5%); electrospray mass spectrum: m/z = 1177, 1096, 950, 869 and 717; calc. for $C_{32}H_{44}{}^{79}Br_2{}^{101}Ru^{121}Sb_4$ 1171, $C_{32}H_{44}{}^{79}Br^{101}Ru^{121}Sb_4$ 1092, C_{24}-$H_{33}{}^{79}Br_2{}^{101}Ru^{121}Sb_3$ 943, $C_{24}H_{33}{}^{79}Br^{101}Ru^{121}Sb_3$ 867 and C_{16}-$H_{22}{}^{79}Br_2{}^{101}Ru^{121}Sb_2$ 715; *trans*-$[RuI_2(SbMe_2Ph)_4]BF_4$, dark brown solid (Found: C, 28.1; H, 2.9. Calc. for $C_{32}H_{44}BF_4$-I_2RuSb_4: C, 28.3; H, 3.2%); electrospray mass spectrum: m/z = 1041, 916 and 687; calc. for $C_{24}H_{33}I_2{}^{101}Ru^{121}Sb_3$ 1039, $C_{24}H_{33}I^{101}Ru^{121}Sb_3$ 912 and $C_{16}H_{22}I^{101}Ru^{121}Sb_2$ 684; and *trans*-$[RuI_2(AsMe_2Ph)_4]BF_4$ (Found: C, 32.6; H, 3.5. Calc. for $C_{32}H_{44}As_4BF_4I_2Ru$: C, 32.8; H, 3.8%); electrospray mass spectrum: m/z = 901, 774, 719 and 592; calc. for $C_{24}H_{33}As_3I_2{}^{101}Ru$ 901, $C_{24}H_{33}As_3I^{101}Ru$ 774, $C_{12}H_{22}As_2I_2{}^{101}Ru$ 719 and $C_{16}H_{22}$-$As_2I^{101}Ru$ 592.

Crystallography

Details of the crystallographic studies are presented in Table 5. Data were collected on a Rigaku AFC7S diffractometer equipped with Mo-Kα radiation (λ = 0.710 69 Å) and a graphite monochromator. Selected crystals were mounted on glass fibres following oil immersion and held at 150 K using an Oxford Cryosystems low-temperature device. Lorentz-polarisation corrections and any correction for the small amount of decay were applied during data reduction. Structure solution was by means of SHELXS 86[15] and full-matrix least-squares refinement on F was carried out with the TEXSAN package.[16] A few of the thermal ellipsoids of the carbon atoms were suggestive of disorder although individual atom sites could not be recognised and where the non-positive definite condition arose those atoms were treated as isotropic. This problem could be associated with the empirical absorption corrections used and the rather large μ values or genuine disorder. Hydrogen atoms were usually included in the model in calculated positions [d(C–H) = 0.95 Å]. Other details for individual structures are as follows.

***trans*-[RuBr$_2$(SbMe$_2$Ph)$_4$].** Dark purple crystals were obtained from liquid diffusion of ethanol into dichloromethane. All the C atoms were treated as anisotropic.

***trans*-[RuI$_2$(AsMe$_2$Ph)$_4$].** Red crystals were obtained as above. All the C atoms except four were treated as anisotropic.

[Ru$_2$Br$_5$(SbMe$_2$Ph)$_4$]. Purple rhomb-shaped crystals were obtained as above during attempts to grow crystals of *trans*-$[RuBr_2(SbMe_2Ph)_4]$. The N(z) test favoured the centric distribution and the analysis was carried out in the space group $C2/c$. All the C atoms were treated as anisotropic.

[Ru$_2$I$_3$(PMe$_2$Ph)$_6$][CF$_3$SO$_3$]. Crystals were obtained by liquid diffusion of hexane into a dichloromethane solution of the bulk material. The cation readily emerged during the structure solution and all C atoms were treated as anisotropic. No H atoms were included in the model. In later Fourier maps four small (*ca.* 3–4 e Å^{-3}) peaks were observed. Three of these were interpreted as the S atoms of partial and disordered $[CF_3SO_3]^-$ anions as they showed clusters of adjacent peaks (oxygens) at appropriate distances; the fourth showing no surrounding peaks was interpreted as a partial occupancy iodide anion. The atom population (with a fixed isotropic thermal parameter) refined to the small value 0.060(3). Three O atoms were included but the C and F atoms of the triflate were not satisfactorily modelled.

CCDC reference number 186/712.

Acknowledgements

We thank the EPSRC for support and funds to purchase the X-ray diffractometer, and for access to the Chemical Database Service at Daresbury. We also thank Dr. G. Reid for determining the structure of $[RuI_2(AsMe_2Ph)_4]$ and Dr. S. R. Preece for some preliminary studies.

References

1 R. A. Cipriano, W. Levason, R. A. S. Mould, D. Pletcher and M. Webster, *J. Chem. Soc.*, *Dalton Trans.*, 1990, 339.
2 R. A. Cipriano, W. Levason, R. A. S. Mould, D. Pletcher and M. Webster, *J. Chem. Soc.*, *Dalton Trans.*, 1990, 2609.
3 N. R. Champness, W. Levason, R. A. S. Mould, D. Pletcher and M. Webster, *J. Chem. Soc.*, *Dalton Trans.*, 1991, 2777; N. R. Champness, C. S. Frampton, W. Levason and S. R. Preece, *Inorg. Chim. Acta*, 1995, **233**, 43.
4 P. W. Armit, A. S. F. Boyd and T. A. Stephenson, *J. Chem. Soc.*, *Dalton Trans.*, 1975, 1663.
5 J. Chatt and R. G. Hayter, *J. Chem. Soc.*, 1961, 896.
6 H. Werner and J. Gotzig, *J. Organomet. Chem.*, 1985, **284**, 73; J. Gotzig, R. Werner and H. Werner, *J. Organomet. Chem.*, 1985, **285**, 99.
7 C. M. Duff and G. A. Heath, *J. Chem. Soc.*, *Dalton Trans.*, 1991, 2401; *Inorg. Chem.*, 1991, **30**, 2528.
8 N. J. Holmes, A. R. J. Genge, W. Levason and M. Webster, *J. Chem. Soc.*, *Dalton Trans.*, 1997, 2331.
9 N. R. Champness, W. Levason, S. R. Preece, M. Webster and C. S. Frampton, *Inorg. Chim. Acta*, 1996, **244**, 65.
10 R. J. Judd, R. Cao, M. Biner, T. Armbruster, H.-B. Burgi, A. E. Merbach and A. Ludi, *Inorg. Chem.*, 1995, **34**, 5080.
11 N. R. Champness, W. Levason and M. Webster, *Inorg. Chim. Acta*, 1993, **208**, 189.
12 N. R. Champness, W. Levason, D. Pletcher and M. Webster, *J. Chem. Soc.*, *Dalton Trans.*, 1992, 3243.
13 C. M. Che, S. S. Wong and K. C. Poon, *Inorg. Chem.*, 1985, **24**, 1601.
14 G. A. Heath, D. C. R. Hockless and B. D. Yeomans, *Acta Crystallogr.*, *Sect. C*, 1996, **52**, 854.
15 G. M. Sheldrick, SHELXS 86, Program for crystal structure solution, *Acta Crystallogr.*, *Sect. A*, 1990, **46**, 467.
16 TEXSAN, Single crystal structure analysis software, version 1.7-1, Molecular Structure Corporation, The Woodlands, TX, 1995.

Received 4*th June* 1997; *Paper* 7/03897F